Microchemical Journal 141 (2018) 80–86

Contents lists available at ScienceDirect

Microchemical Journal

journal homepage: www.elsevier.com/locate/microc

High-throughput chemometrically assisted flow-injection method for the simultaneous determination of multi-antiretrovirals in water

Lesly Paradina Fernández[a,b], Romina Brasca[a,b,c], Mirta R. Alcaráz[a,b], María J. Culzoni[a,b,*]

[a] Laboratorio de Desarrollo Analítico y Quimiometría (LADAQ), Cátedra de Química Analítica I, Facultad de Bioquímica y Ciencias Biológicas, Universidad Nacional del Litoral, Ciudad Universitaria, 3000 Santa Fe, Argentina

[b] Consejo Nacional de Investigaciones Científicas y Técnicas (CONICET), Godoy Cruz 2290, 1425 Buenos Aires, Argentina

[c] Programa de Investigación y Análisis de Residuos y Contaminantes Químicos (PRINARC), Facultad de Ingeniería Química, Universidad Nacional del Litoral, Santiago del Estero 2654, 3000 Santa Fe, Argentina

ARTICLE INFO

Keywords:
Antiretroviral
pK_a
Quantitation
FIA-DAD
MCR-ALS
Environmental samples

ABSTRACT

This work is focused on the simultaneous determination of different nucleosides (lamivudine, abacavir, zidovudine) and non-nucleoside (nevirapine, efavirenz) reverse transcriptase inhibitors (antiretrovirals) in river, tap and well water by pH-gradient flow-injection analysis with diode-array detection (FIA-DAD) and further multivariate curve resolution-alternating least square (MCR-ALS) processing. Previous to the development of the analytical method with quantitative purpose, the acid-base characterization was conducted for all the analytes by determination of the experimental pK_a. The pK_a values, obtained by UV spectrometric titration coupled to MCR-ALS data modeling, were in agreement with those found in the literature, and, interestingly, a non-reported pK_a of 12.27 was identified for nevirapine. Eventually, the analytical method was developed and its performance on the quantitation of the antiretrovirals was evaluated through its application to validation and environmental samples. The recovery studies showed values between 85 and 115% with relative errors of prediction below 10%. The figures of merit were satisfactory for all the studied drugs, with limits of detection between 25 and 40 $\mu g\,L^{-1}$. Therefore, the proposed method, which is based on the generation of high-throughput data, is a simple and suitable alternative to determine the concentration of antiretroviral drugs in complex matrices, without pre-concentration or extraction steps. Additionally, MCR-ALS demonstrated to be a useful tool for solving mixtures of analytes with high spectral overlapping, in the presence of unknown interferences.

1. Introduction

The acquired immune deficiency syndrome (AIDS) caused by the human immunodeficiency virus (HIV) is one of the greatest lethal diseases in the world. It is estimated that causes about 1 million deaths per year worldwide [1,2]. The most widely used treatment, known as highly active antiretroviral therapy, combines at least two nucleoside analogue reverse transcriptase inhibitors, such as lamivudine (3TC), abacavir (ABC) or zidovudine (AZT), with one non-nucleoside reverse transcriptase inhibitor, such as nevirapine (NVP) or efavirenz (EFV), in a fixed dose combination [3]. The synergistic action provided by this therapy has allowed reducing both mortality and morbidity rates among HIV-infected people, improving their life quality.

Antiretroviral drugs are considered emerging contaminants since they were found in the environment and can cause adverse ecological and/or human health effects. However, they are not usually monitored due to the lack of regulations [4]. Although these drugs are generally present at rather low levels (from $ng\,L^{-1}$ to $\mu g\,L^{-1}$) in wastewater and surface waters [5–7], the continuous input can increase the concentrations bringing potential negative effects on the environment, e.g., antimicrobial resistance and toxicity to sensitive aquatic organisms. Their simultaneous determination in environmental samples, as well as in pharmaceutical dosage, biological fluids, animal tissue, synthetic mixtures, has been performed by near-infrared spectroscopy [8], high performance liquid chromatography with diode array detection (HPLC-DAD) [9], U-HPLC with tandem mass spectrometry detection (MS/MS) [10] and pH-gradient flow injection analysis (FIA) with DAD [11].

The aforementioned antiretrovirals (3TC, ABC, AZT, NVP and EFV) exhibit acid-base properties that cause UV spectral changes when variations in the pH of the medium are produced. It is known that the pK_a of the analytes plays an important role from an analytical point of view. Therefore, prior to the development of a pH-gradient with spectral

* Corresponding author at: Laboratorio de Desarrollo Analítico y Quimiometría (LADAQ), Cátedra de Química Analítica I, Facultad de Bioquímica y Ciencias Biológicas, Universidad Nacional del Litoral, Ciudad Universitaria, 3000 Santa Fe, Argentina.
E-mail address: mculzoni@fbcb.unl.edu.ar (M.J. Culzoni).

https://doi.org/10.1016/j.microc.2018.05.011
Received 15 March 2018; Received in revised form 7 May 2018; Accepted 8 May 2018
Available online 09 May 2018
0026-265X/

Table 1
Summary and brief description of published works with experimental apparent pK_a values of antiretroviral drugs.

Pharmaceutical drug	Method	Experimental procedure			pK_a	Ref.
		pH range	T (°C)	I (mol L^{-1})		
3TC	–	–	–	–	4.3	[31]
	Capillary electrophoresis	2–11	25	0.05 (NaCl)	4.24	[14]
	UV spectroscopy	2–13	25	0.06 (KCl)	4.19 (2)[a]	[This work]
ABC	–	–	–	–	5.1	[31]
	Capillary electrophoresis	2–11	25	0.05 (NaCl)	5.04	[14]
	UV spectroscopy	2–13	25	0.06 (KCl)	5.20 (1) [a]	[This work]
AZT	–	–	–	–	9.7	[31]
	FIA-DAD	3.5–10.5	–	–	9.55	[23]
	Potentiometry	–	–	–	9.85	[13]
	Differential scanning potentiometry	–	25	–	9.42	[12]
	UV spectroscopy	2–13	25	0.06 (KCl)	9.90 (1) [a]	[This work]
NVP	–	–	–	–	2.8	[31]
	Solubility	1–6	25	–	2.65	[32,33]
	UV spectroscopy	2–13	25	0.06 (KCl)	2.85 (1)[a] 12.27 (2)[a],12.27 (3)[b]	[This work]
EFV	–	–	–	–	10.2	[31]
	Solubility	1–13	–	–	10.1	[15]
	UV spectroscopy	1–13	–	0.15	10.2[c]	
	UV spectroscopy	2–13	25	0.06 (KCl)	10.11 (2)[a]	[This work]

[a] pK_a value calculated by MCR-ALS. Experimental standard deviation in the last significant figure in parentheses.
[b] pK_a value calculated by sigmoidal curve fitting using the wavelength of maximum absorbance corresponding to the acid species. Experimental standard deviation in the last significant figure in parentheses.
[c] Thermodynamic pK_a.

detection method, an in-depth bibliographic search related to the pK_a values of the five herein analyzed drugs was conducted and summarized in Table 1. It is clear that the available information is scarce or incomplete, especially due to the lack of description of the experimental conditions in which they were determined.

Analytical methods used for pK_a determinations of several drugs include potentiometry [12,13], capillary electrophoresis (CE) with DAD [14], UV–Vis spectroscopy [15] and FIA-DAD [11], among others. The most commonly used estimator for the pK_a is the well-known Henderson-Hasselbalch equation [16], whereas chemometric resolution of spectrophotometric second-order data constitutes an alternative way of calculation. In this sense, MCR-ALS [17–19] has been widely applied to calculate pK_a from second-order data gathered by different instrumentations in several research fields, i.e. UV spectroscopy [20,21], FIA-DAD [22,23], CE-DAD [24] and fluorescence spectroscopy [20,25].

In this work, the apparent pK_a values of 3TC, ABC, AZT, NVP and EFV were determined by spectrophotometric titrations and chemometric data analysis. Then, based on this physicochemical information, a FIA-DAD method with MCR-ALS modeling for the simultaneous quantitation of these five drugs in aqueous environmental samples was developed.

2. Materials and methods

2.1. Reagents and solutions

3TC, ABC, AZT, NVP and EFV were kindly supplied by Laboratorio DOSA S.A (Buenos Aires, Argentina). Potassium chloride (KCl) was purchased from Merck (New York, USA). Hydrochloric acid (37%, HCl), potassium hydroxide (KOH), sodium hydroxide (NaOH), phosphoric acid (85%, H_3PO_4) and sodium phosphate dibasic (Na_2HPO_4) were purchased from Anedra (San Fernando, Argentina). All reagents were of analytical grade. HPLC grade methanol (MeOH) was purchased from Biopack (Buenos Aires, Argentina). Ultrapure water was obtained from a Millipore system (Bedford, USA).

Five 1000 μg mL^{-1} stock solutions were prepared by dissolving the appropriate amounts of 3TC and ABC in ultrapure water and NVP, AZT and EFV in MeOH. Stock solutions were stored in the darkness at 4 °C. The working solutions were prepared by adequate dilution of the stock solution in the corresponding solvent to reach a final concentration of 100 μg mL^{-1}. The 0.2 mol L^{-1} phosphate carrier solution was prepared by transferring the suitable aliquot of H_3PO_4 to a 500.0 mL volumetric flask, adjusting the pH to 2.45 with 8.0 mol L^{-1} NaOH, and completing to the mark with ultrapure water. The 1.0 mol L^{-1} sample buffer was prepared by dissolving g the appropriate amount of Na_2HPO_4 in ultrapure water, adjusting the pH to 11.00 with 1.0 mol L^{-1} NaOH, and completing to 100.0 mL with ultrapure water.

The aqueous environmental samples were obtained from different regions of Argentina and stored at 4 °C until the experiments were performed. Well water and tap water samples were gathered from Coronda City and Santa Fe City, respectively, both located at the province of Santa Fe. Five river samples were collected from different districts of the province of Santa Fe (Santa Fe River, Cuculucito River, Colastiné River, Salado River and San Javier River) and three samples were taken from different rivers located at San Luis, Entre Rios and Buenos Aires provinces (Boca del Río River, Gualeguay River and Lujan River, respectively).

2.2. Spectrophotometric titrations

2.2.1. Apparatus

When performing the spectrophotometric titrations, the pH was monitored with an Orion 410A (Massachusetts, USA) potentiometer equipped with an Orion ROSS Ultra (Massachusetts, USA) combined glass electrode. The absorption spectra were registered every 0.5 nm in the spectral range of 200–400 nm using a Perkin Elmer Lambda 20 UV–Vis spectrophotometer (Massachusetts, USA) in a 1.00 cm-quartz cuvette at a scan rate of 480 nm/min using 2 nm slit widths. The matrices comprised 401 data points in the spectral dimension, while the pH mode ranged from 25 to 32 depending on the experimental procedure.

2.2.2. Data generation

All measurements were performed in solutions with 0.06 mol L^{-1} initial ionic strength (given by KCl 3 mol L^{-1}) at 25 °C using a circulating water bath to control the temperature. The spectrophotometric titration experiments were conducted in acidified (pH~2) solutions containing 10 μg mL^{-1} of each analyte. The general procedure involved

Table 2
Determination of 3TC, ABC, AZT, NVP and EFV in validation samples by FIA-DAD.

Sample	3TC[a]		ABC[a]		AZT[a]		NVP[a]		EFV[a]	
	Nominal	Predicted[b]	Nominal	Predicted[b]	Nominal	Predicted[b]	Nominal	Predicted[b]	Nominal	Predicted[b]
1	450	476 (9) [106]	350	381 (4) [109]	150	155 (4) [103]	250	234 (8) [94]	450	451 (2) [100]
2	350	345 (6) [99]	450	461 (5) [102]	250	275 (7) [110]	350	356 (3) [102]	150	140 (7) [93]
3	300	299 (7) [100]	300	301 (9) [100]	300	301 (7) [100]	300	302 (5) [101]	300	299 (6) [100]
4	250	247 (1) [99]	150	168 (9) [112]	350	316 (6) [90]	450	449 (9) [100]	250	264 (2) [106]
5	150	139 (5) [93]	250	250 (1) [100]	450	463 (6) [103]	150	163 (8) [109]	350	363 (4) [104]
REP%[c]	4.2		5.3		6.0		3.3		3.1	

[a] All the concentrations are given in $\mu g\,L^{-1}$.

[b] All the values are expressed as the average of the corresponding replicates. Experimental standard deviations are shown in the last significant figure in parentheses, and the recoveries are in square brackets (%).

[c] REP%: relative error of prediction, $REP = 100\frac{RMSE}{\bar{c}}$, where $\bar{c}$ is the mean calibration concentration and $RMSE = \sqrt{\frac{1}{I}\sum_1^I (c_{nom} - c_{pred})^2}$ for $I = 13$.

the addition of small aliquots of $0.1\,mol\,L^{-1}$, $1.0\,mol\,L^{-1}$ and $3.0\,mol\,L^{-1}$ KOH, as appropriate, to 50.0 mL of the stirred initially acid solution, in order to obtain small pH increments. Once each pH value was reached, the corresponding spectrum was acquired by extracting 2.0 mL of the solution from the vessel, which were then restored to the original solution, until reaching pH~13. At the end of the titration, one spectrum for each pH value was recorded.

For each analyte, reference absorption spectra of pure acid and basic species were obtained from experiments done at selected pH conditions: pH 2.0 and 13.0.

2.2.3 pK_a determinations.

pK_a determinations were conducted by MCR-ALS modeling of data matrices built with the antiretroviral spectra recorded at each pH value. MCR-ALS performs the bilinear decomposition of a **D** matrix according to:

$$\mathbf{D}_{IxJ} = \mathbf{C}_{IxN} \times \mathbf{S}^{\mathbf{T}}_{NxJ} + \mathbf{E}_{IxJ} \quad (1)$$

where **D** ($I \times J$) is the measured data matrix that includes the experimental UV spectra (J) at each pH value (I). **C** ($I \times N$) comprises the concentration profiles of the N species present in the system, and $\mathbf{S}^{\mathbf{T}}$ ($N \times J$) the associated spectra of each specie. **E** contains the residuals of the model [26].

The chemical rank of individual matrices was estimated by singular value decomposition (SVD) [27]. The estimations needed to initialize the ALS optimization were obtained by a procedure based on the Simple-to-use Interactive Self-modeling Mixture Analysis (SIMPLISMA) [28]. Decomposition of **D** was achieved by iterative least-squares minimization of ||**E**||, under suitable constrained conditions, i.e. non-negativity in spectral mode, and closure and non-negativity in concentration mode.

2.3. FIA-DAD procedure

2.3.1. Apparatus

The FI system was developed using an Agilent 1100 Series LC instrument (Waldbronn, Germany). The carrier solution consisted in $0.2\,mol\,L^{-1}$ H_3PO_4/NaH_2PO_4 (pH = 2.45) and the sample buffer was $0.1\,mol\,L^{-1}$ Na_3PO_4/Na_2HPO_4 (pH = 11.00). The carrier solution was pumped through an 800 mm length and 0.5 mm i.d. flexible mixing coil flowing at $0.3\,mL\,min^{-1}$. The temperature was set at 25 °C. The spectra were registered every 1 nm in the range of 230–400 nm during 1.9 min. Thus, the data matrices were of size 143 × 171 for the temporal and spectral dimensions, respectively.

2.3.2. Calibration and validation samples

For each analyte, a calibration set of six samples was prepared in triplicate by transferring appropriate aliquots of the $100\,\mu g\,mL^{-1}$ working solutions to 10.0 mL volumetric flasks. For AZT, NVP and EFV, the transferred aliquots were dried with nitrogen flow to evaporate the MeOH and sonicated with approximately 5 mL of water for 10 min. Then, 1.0 mL of $1.0\,mol\,L^{-1}$ sample buffer was added to the 10.0 mL volumetric flasks, which were finally completed to the mark with ultrapure water. The final concentration of the calibration samples were in the range of 50–500 $\mu g\,L^{-1}$ for each analyte. At last, 1.0 mL aliquots of each sample were transferred to injection vials and 100.0 µL were injected into the FI system.

A 5-sample validation set composed of mixtures of the five analytes was built in duplicate, except for sample 3 which was prepared in quintuplicate, considering concentrations different than those used in the calibration and following a random design (Table 2).

2.3.3. Aqueous environmental samples

Environmental samples were prepared by spiking river, tap and well water with each analyte in five different concentration levels (Table 3). The solutions were centrifuged at 3000 rpm for 10 min and filtered through 0.2 µm nylon membranes. The sample preparation was similar to the above described, but completing to the mark with river, tap or well water, as appropriate. This procedure was performed in duplicate.

2.4. Software

MCR-ALS was implemented in MATLAB 7.6 [29]. The algorithms for applying MCR-ALS are available online at http://www.mcrals.info/.

3. Results and discussion

3.1. General considerations

It is well-known that the pK_a strongly depends on the temperature, ionic strength and dielectric constant of the solution [30]. Nevertheless, some works reporting the determination of the pK_a values of antiretroviral drugs avoid maintaining these parameters controlled during the experiments (or did not informed them), as can be seen in Table 1. It is worth noting that determinations at constant ionic strength require the preparation of different solutions for each measurement, which is impractical from experimental and financial points of view, mainly due to the high solvent consumption, waste generation, analysis time and introduction of systematic errors.

Considering that in this work the pK_a determination was done following an analytical purpose, the experimental conditions were established in view of the development of a quantitative method for antiretrovirals based on FIA-DAD. Therefore, in the present work, the temperature was set at 25 °C and kept constant during the titration experiments, whereas an ionic strength of $0.06\,mol\,L^{-1}$ was established for each sample solution at the beginning of the titrations.

Table 3
Recovery study of 3TC, ABC, AZT, NVP and EFV in spiked environmental aqueous samples.

Sample	3TC[a]		ABC[a]		AZT[a]		NVP[a]		EFV[a]	
	Nominal	Found[b]	Nominal	Found[b]	Nominal	Found[b]	Nominal	Found[b]	Nominal	Found[b]
Well water[c]	150	172 (3) [115]	250	274 (8) [109]	450	471 (9) [105]	150	142 (2) [95]	350	326 (8) [93]
Tap water[d]	450	453 (1) [101]	350	314 (8) [90]	150	171 (6) [114]	250	284 (4) [114]	450	469 (7) [104]
River water[e]	450	445 (3) [99]	350	343 (1) [98]	150	155 (4) [103]	250	278 (8) [111]	450	439 (6) [98]
River water[f]	300	282 (3) [94]	300	296 (4) [99]	300	277 (2) [93]	300	285 (3) [95]	300	332 (1) [111]
River water[g]	250	247 (1) [99]	150	137 (2) [92]	350	356 (4) [102]	450	457 (6) [102]	250	230 (6) [92]
River water[h]	350	313 (9) [89]	450	473 (4) [105]	250	283 (7) [113]	350	349 (6) [100]	150	158 (4) [105]
River water[i]	300	289 (6) [96]	300	289 (2) [97]	300	290 (1) [97]	300	307 (1) [102]	300	304 (6) [101]
River water[j]	250	244 (7) [98]	150	171 (4) [114]	350	345 (1) [99]	450	383 (6) [85]	250	245 (1) [98]
River water[k]	450	449 (4) [100]	350	364 (8) [104]	150	145 (6) [96]	250	228 (2) [91]	450	448 (7) [99]
River water[l]	350	331 (2) [95]	450	461 (8) [103]	250	219 (5) [88]	350	307 (4) [88]	150	162 (1) [108]
REP%[m]	5.1		6.1		7.3		9.8		5.5	

[a] All the concentrations are given in μg L^{-1}.
[b] All the values are expressed as the average of the duplicates. Experimental standard deviations are shown in the last significant figure, in parentheses, and the recoveries are in square brackets (%).
[c] From Coronda City (Santa Fe, Argentina).
[d] Santa Fe City (Santa Fe, Argentina).
[e] Boca del Río River (San Luis, Argentina).
[f] Santa Fe River (Santa Fe, Argentina).
[g] Cuculucito River (Santa Fe, Argentina).
[h] Ualeguay River (Entre Ríos, Argentina).
[i] Lujan River (Buenos Aires, Argentina).
[j] San Javier River (Santa Fe, Argentina).
[k] Colastiné River (Santa Fe, Argentina).
[l] Salado River (Santa Fe, Argentina).
[m] REP%: relative error of prediction, $REP = 100\frac{RMSE}{\bar{c}}$, where $\bar{c}$ is the mean calibration concentration and $RMSE = \sqrt{\frac{1}{I}\sum_1^I (c_{nom} - c_{pred})^2}$ for $I = 20$.

3.2. Spectrophotometric titrations

The absorption spectra of 3TC, ABC, AZT, NVP and EFV in aqueous solution as a function of the pH are shown in Fig. 1. Notable pH-dependent spectral variations can be observed for all analytes. For example, 3TC at acid pH presents maximum absorbance at 280 nm but there is a hypsochromic shift to 271 nm at basic pH with a prominent decrease in intensity (Fig. 1A). The main spectral variation for ABC is observed from 295 nm to 285 nm when varying from acid to basic conditions (Fig. 1B). AZT shows a unique maximum absorbance at 266 nm, which only changes in intensity, being the major absorbance values at acid pH (Fig. 1C). For the particular case of NVP, different isosbestic points emerge with raising pH values, which are correlated with the fact that different acid-base equilibriums are evolving as the pH changes. These observations suggest the presence of different acid-base equilibriums and, in consequence, the existence of different pKa values, even though only one is reported in the literature [31–33] (Fig. 1D). EFV exhibits an intense maximum absorption band at 247 nm in acid conditions which decreases with pH increments and, at the same time, a new band arises at 266 nm (Fig. 1E).

3.3. pK_a determinations

The chemometric resolution of the generated absorbance-pH data was performed for each analyte. The first step in the MCR resolution was the estimation of the number of components involved in the systems. In this sense, the number of factors estimated using SVD were three for NVP and two for 3TC, ABC, AZT and EFV. In order to optimize the data matrix resolution and obtain final solutions with chemical meaning, constraints such as non-negativity and closure, which assures the mass balance of the species involved in the equilibrium, were applied.

The tridimensional plot of a NVP data matrix and its MCR-ALS resolution is depicted in Fig. 2. It can be appreciated that the obtained spectral profiles (Fig. 2B) are in agreement with the experimental pure spectra, indicating the good performance of MCR-ALS in the resolution of this kind of data. In the case of the species distribution diagram (Fig. 2C), a sigmoidal fit of the data and two pK_a values, i.e. 2.85 and 12.27, were observed. It is important to highlight that the proposed methodology allowed finding pK_{a2} value for NVP, which was not previously reported in the literature. In order to confirm the value of new pKa_2, a sigmoidal curve fitting of the measured absorbance, at a specific wavelength, as function of pH was performed for the NVP acid species followed by pK_a calculation from the inflection point [34]. Both methodologies provided the same calculated value of 12.27 (Table 1). Therefore, the chemometric strategy proved to be a suitable tool in the pK_a determination of antiretroviral drugs. The calculated pK_a values for all the drugs are summarized in Table 1 together with those found in the literature.

3.4. Quantitation of antiretrovirals by FIA-DAD

3.4.1. Validation samples

The quantitation of the analytes in validation and real samples was done for each drug individually. The data processing was performed on an augmented column-wise **D** data matrix that consisted in 385 × 121 data points for temporal and spectral dimensions, respectively. **D** matrix was built by appending the matrix corresponding to a validation sample, the calibration data matrices and one matrix corresponding to the sample of each of the other analytes. Before performing MCR-ALS, the determination of the number of components in the model was carried out based on the previous knowledge of the system, i.e. twelve factors were selected for the validation mixtures (two for each analytes and two for the background). In addition, initial spectral estimations were carried out by analysis of the purest spectra based on the SIMPLISMA methodology [28]. During the ALS optimization the following constraints were applied: non-negativity in concentration and spectral modes, and correspondence between common species in the different matrices.

After MCR-ALS decomposition of **D**, the pseudo-univariate

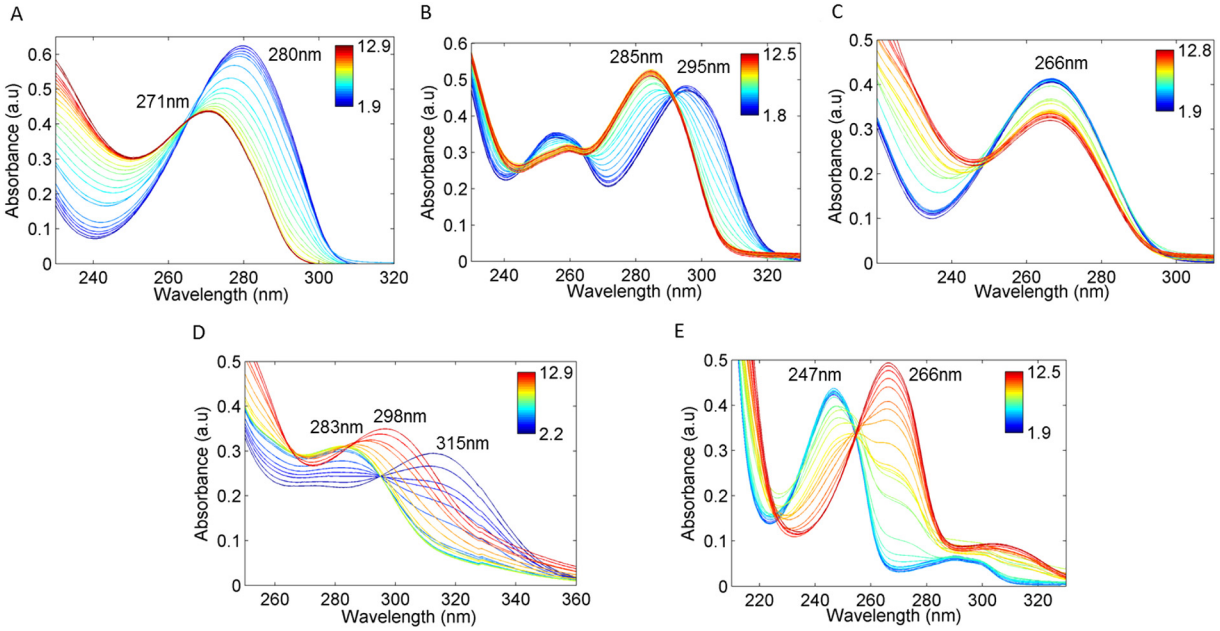

Fig. 1. UV absorption spectra of 10 μg mL^{-1} aqueous solutions of (A) 3TC, (B) ABC (C) AZT, (D) NVP and (E) EFV at different pH values.

regression of area against concentration for each analyte was built with the concentration information of the calibration samples contained in **C**. In all cases, the calculations were performed using the basic species, due to their higher sensitivity in the whole concentration range.

Taking into account the high spectra overlapping between species in the sample mixtures (Fig. 3), an appropriate chemometric resolution that would allow the simultaneous quantitation of these drugs was pursued. To evaluate the quality of the modeling, a comparison between the pure experimental spectra ($\mathbf{s}_1$) and MCR-ALS retrieved spectral profile ($\mathbf{s}_2$) was carried out. To quantitate the degree of spectral overlap (s_{12}) the following expression was employed:

$$s_{12} = \frac{\|\mathbf{s}_1^{\mathrm{T}}\mathbf{s}_2\|}{\|\mathbf{s}_1\|\,\|\mathbf{s}_2\|} \tag{2}$$

The value of s_{12} ranges from 0 to 1, corresponding to the extreme situation of no overlapping and complete overlapping [35]. The s_{12} figures obtained for basic and acid species were: 0.9972 and 0.9966 for 3TC; 0.9960 and 0.9909 for ABC; 0.9929 and 0.9937 for AZT; 0.9904 and 0.9760 for NVP and 0.9968 and 0.9962 for EFV. A high overlap between normalized pure experimental spectra and the retrieved spectral profiles were observed, except for NVP, probably because its pK_{a1} (2.8) is very close to the pH of the carrier solution (2.45).

Table 2 summarizes the predicted concentrations for the validation samples. As can be seen, satisfactory recovery values between 90 and

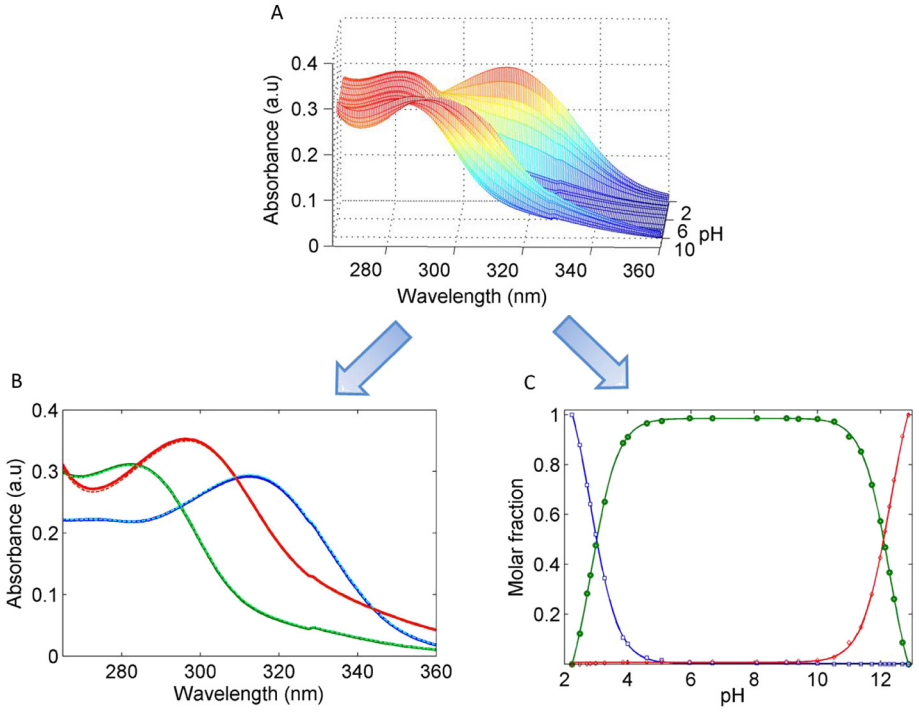

Fig. 2. (A) 3D plot for NVP data matrix, (B) spectral profile achieved from MCR-ALS (solid lines) and experimental pure spectra (dotted lines), and (C) species distribution curves obtained by MCR-ALS (the experimental values are indicated in circles and the fitted curves are showed in blue, green and red solid lines for acid, intermediate and basic forms, respectively). (For interpretation of the references to colour in this figure legend, the reader is referred to the web version of this article.)

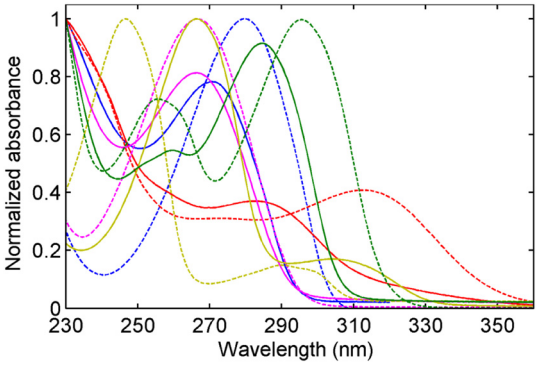

Fig. 3. UV spectra of acid (dotted lines) and basic species (solid lines) of 3TC (blue), ABC (green), AZT (violet), NVP (red) and EFV (yellow). (For interpretation of the references to colour in this figure legend, the reader is referred to the web version of this article.)

Table 4
Analytical figures of merit.

Figures of merit	3TC	ABC	AZT	NVP	EFV
Sensitivity (AU μg^{-1} L)	0.072	0.14	0.059	0.11	0.050
Analytical sensitivity (μg^{-1} L)	14	27	12	22	10
LOD[a] ($\mu g\,L^{-1}$)	25	40	40	25	39
LOQ[b] ($\mu g\,L^{-1}$)	74	120	122	77	120

[a] LOD: limit of detection calculated according to Ref [37].
[b] LOQ: limit of quantitation calculated as LOD × 10/3.3.

112%, and relative errors of prediction (REP %) below 10%, were obtained. With the aim of proving that the recoveries were not different than 100%, a statistical analysis was applied assuming a hypothesis test: H_0: $\overline{R}_{exp} = 100\%$ and H_1: $\overline{R}_{exp} \neq 100\%$. The experimental t_{exp} values were estimated according to:

$$t_{exp} = |100 - \overline{R}_{exp}| \frac{\sqrt{n}}{S_R} \quad (3)$$

where $\overline{R}_{exp}$ is the average experimental recovery and s_R the standard deviation of the recoveries. The recoveries are considered statistically different than 100% when t_{exp} value exceed the critical $t_{(\alpha,\upsilon)}$ value at level α, $\upsilon = n–1$ grade of freedom and n samples [36]. For a 95% confidence level, the experimental t_{exp} value for all drugs in the validation samples were lower than the critical value $t_{(0.025,12)}$, thus, H_0 is accepted, indicating the accuracy of the method.

In analytical chemistry, figures of merit (FOMs) are numerical parameters useful to compare the relative performances of different analytical methodologies and to discriminate between their detection capabilities. Table 4 summarizes the FOMs estimated according to Bauza et al. [37]. As can be seen, acceptable values were obtained for all the analytes with limits of detection (LOD) between 25 and 40 $\mu g\,L^{-1}$, and limits of quantitation (LOQ) between 74 and 122 $\mu g\,L^{-1}$. Usually, the levels of these drugs in environmental samples are in the order of the ng L^{-1}, but recent studies report concentrations for 3TC in wastewater and rivers of Kenya in the range of 30–60 $\mu g\,L^{-1}$ and 167 $\mu g\,L^{-1}$, respectively [38]. Similar results have been reported for AZT (6.9–53 $\mu g\,L^{-1}$) and EFV (20–34 $\mu g\,L^{-1}$) in wastewater collected in South Africa by Abafe et al. [39]. In this sense, the proposed methodology, which does not require pre-concentration steps, becomes a suitable alternative to simultaneously monitor the levels of the five antiretroviral drugs in environmental aqueous matrices by generation of high-throughput spectroscopic data.

3.4.2. Environmental water samples

In order to evaluate the applicability of the developed methodology, a recovery study was conducted for the determination of the five analytes on spiked environmental samples, which did not show evidences of 3TC, ABC, AZT, NVP and EFV residues. The data matrices were processed following the procedure applied for the validation set, but considering one or two more components, as appropriate, associated with the interferences present in the samples.

Table 3 displays the recoveries obtained for each drug in ten environment aqueous matrices from different regions of Argentina. The experimental t_{exp} values are lower than the critical $t_{(0.025,19)}$ value for all drugs; therefore, the recoveries are not statistically different than 100%, suggesting the proposed method is appropriate to simultaneously analyze the five antiretrovirals in environmental aqueous samples.

4. Conclusions

The spectral behavior of the antiretroviral drugs against pH allowed determining their pK_a by spectrophotometric titration and MCR-ALS analysis. All the pK_a values were consistent with the literature data and for the case of NVP a second pK_a value, which was not previously reported, was established.

Taking into account that the presence of emerging contaminants in highly complex environmental samples is of current concern due to the potential occurrence of adverse effects on humans and animals, a method for the simultaneous determination of five antiretrovirals based on the MCR-ALS modeling of FIA-DAD data was developed. It proved to be an inexpensive and fast methodology capable of evaluating the concentration of these drugs in complexes matrices at levels of $\mu g\,L^{-1}$, without resorting to extraction or pre-concentration steps. MCR-ALS second-order data modeling provided satisfactory qualitative and quantitative results, which supported its application to the resolution of highly overlapped spectra in the presence of unmodeled matrix compounds.

Acknowledgements

The authors are grateful to Laboratorios DOSA S.A for supplying the antiretroviral drugs to conduct this study, Universidad Nacional del Litoral (Projects CAI + D 2016-50120150100110LI and 50020150100063LI), CONICET (Consejo Nacional de Investigaciones Científicas y Técnicas, Project PIP-2015 N° 0111) and ANPCyT (Agencia Nacional de Promoción Científica y Tecnológica, Project PICT 2014-0347) for financial support. LPF and MRA thank CONICET for their fellowship.

References

[1] A. Vikram Singh, L.K. Nath, N.R. Pani, Development and validation of analytical method for the estimation of lamivudine in rabbit plasma, J. Pharm. Anal. 1 (2011) 251–257.
[2] UNAIDS, Fact Sheet-world Aids Day, 2017 (2017) http://www.unaids.org/sites/default/files/media_asset/UNAIDS_FactSheet_en.pdf , Accessed date: March 2018.
[3] M. Krishna Matta, N. Rao Pilli, J. Kumar Inamadugu, L. Burugula, S. Rao Jvln, Simultaneous quantitation of lamivudine, zidovudine and nevirapine in human plasma by liquid chromatography–tandem mass spectrometry and application to a pharmacokinetic study, Acta Pharm. Sin. B 2 (2012) 472–480.
[4] M.R. Alcaráz, R. Brasca, M.S. Cámara, M.J. Culzoni, A.V. Schenone, C.M. Teglia, L. Vera-Candioti, H.C. Goicoechea, Multiway calibration approaches to handle problems linked to the determination of emergent contaminants in waters, in: M. Khanmohammadi (Ed.), Current Applications of Chemometrics, NOVA Publishers, New York, 2015, pp. 135–154.
[5] E. Ngumba, P. Kosunen, A. Gachanja, T. Tuhkanen, A multiresidue analytical method for trace level determination of antibiotics and antiretroviral drugs in wastewater and surface water using SPE-LC-MS/MS and matrix-matched standards, Anal. Methods 8 (2016) 6720–6729.
[6] T.P. Wood, C.S.J. Duvenage, E. Rohwer, The occurrence of anti-retroviral compounds used for HIV treatment in South African surface water, Environ. Pollut. 199 (2015) 235–243.
[7] J. Funke, C. Prasse, T.A. Ternes, Identification of transformation products of antiviral drugs formed during biological wastewater treatment and their occurrence in the urban water cycle, Water Res. 98 (2016) 75–83.
[8] S. Grangeiro Junior, L. de Moura França, M.F. Pimentel, M.M. Albuquerque, D.P. de

Santana, A.K.M. Santana, J.A.L. Souza, S.S. Simões, A process analytical technology approach for the production of fixed-dose combination tablets of zidovudine and lamivudine using near infrared spectroscopy and chemical images, Microchem. J. 118 (2015) 252–258.
[9] S.T. Pynnönen, T.A. Tuhkanen, Simultaneous detection of three antiviral and four antibiotic compounds in source-separated urine with liquid chromatography, J. Sep. Sci. 37 (2014) 219–227.
[10] P. Mu, N. Xu, T. Chai, Q. Jia, Z. Yin, S. Yang, Y. Qian, J. Qiu, Simultaneous determination of 14 antiviral drugs and relevant metabolites in chicken muscle by UPLC–MS/MS after QuEChERS preparation, J. Chromatogr. B (2016) 1023–1024 (17–23).
[11] A. Checa, R. Oliver, J. Saurina, S. Hernández-Cassou, Flow-injection spectrophotometric determination of reverse transcriptase inhibitors used for acquired immuno deficiency syndrome (AIDS) treatment, Anal. Chim. Acta 572 (2006) 155–164.
[12] M.A. Raviolo, M.C. Brinon, Preformulation studies of zidovudine derivatives: acid dissociation constants, differential scanning calorimetry, thermogravimetry, X-ray powder diffractometry and aqueous stability studies, Sci. Pharm. 79 (2011) 479–491.
[13] S.A. Teijeiro, M.A. Raviolo, M.I. Motura, M.C. Brinon, 3′-Azido-3′-deoxy-5'-O-isonicotinoylthymidine: a novel antiretroviral analog of zidovudine. II. Stability in aqueous media and experimental and theoretical ionization constants, Nucleosides Nucleotides Nucleic Acids 22 (2003) 1789–1803.
[14] M. Shalaeva, J. Kenseth, F. Lombardo, A. Bastin, Measurement of dissociation constants (pKa values) of organic compounds by multiplexed capillary electrophoresis using aqueous and cosolvent buffers, J. Pharm. Sci. 97 (2008) 2581–2606.
[15] S.R. Rabel, M.B. Maurin, S.M. Rowe, M. Hussain, Determination of the pKa and pH-solubility behavior of an Ionizable cyclic carbamate, (S)-6-Chloro-4-(cyclopropylethynyl)-1,4-dihydro-4-(trifluoromethyl)-2H-3,1-benzoxazin-2-one (DMP 266), Pharm. Dev. Technol. 1 (1996) 91–95.
[16] K.A. Hasselbalch, Die Berechnung der Wasserstoffzahl des Blutes aus der freien und gebundenen Kohlensäure desselben, und die Sauerstoffbindung des Blutes als Funktion der Wasserstoffzahl, Biochem. Z. 78 (1916) 112–144.
[17] R. Tauler, Multivariate curve resolution applied to second order data, Chemom. Intell. Lab. Syst. 30 (1995) 133–146.
[18] A.C. Olivieri, On a versatile second-order multivariate calibration method based on partial least-squares and residual bilinearization: second-order advantage and precision properties, J. Chemom. 19 (2005) 253–265.
[19] M.J. Culzoni, H.C. Goicoechea, Determination of loratadine and pseudoephedrine sulfate in pharmaceuticals based on non-linear second-order spectrophotometric data generated by a pH-gradient flow injection technique and artificial neural networks, Anal. Bioanal. Chem. 389 (2007) 2217–2225.
[20] R. Gargallo, M. Vives, R. Tauler, R. Eritja, Protonation studies and multivariate curve resolution on oligodeoxynucleotides carrying the mutagenic base 2-aminopurine, Biophys. J. 81 (2001) 2886–2896.
[21] M. Mirzaei, M. Khayat, A. Saeidi, Determination of para-aminobenzoic acid (PABA) in B-complex tablets using the multivariate curve resolution-alternating least squares (MCR-ALS) method, Sci. Iranica 19 (2012) 561–564.
[22] K. Musil, V. Florianova, P. Bucek, V. Dohnal, K. Kuca, K. Musilek, Development and validation of a FIA/UV-vis method for pK(a) determination of oxime based acetylcholinesterase reactivators, J. Pharm. Biomed. Anal. 117 (2016) 240–246.
[23] A. Checa, V.G. Soto, S. Hernández-Cassou, J. Saurina, Fast determination of pKa values of reverse transcriptase inhibitor drugs for AIDS treatment by using pH-gradient flow-injection analysis and multivariate curve resolution, Anal. Chim. Acta 554 (2005) 177–183.
[24] C.M. Teglia, R. Brasca, L. Vera-Candioti, H.C. Goicoechea, A novel approach based on capillary electrophoresis coupled to augmented multivariate curve resolution-alternating least-squares modeling for the determination of pKa of 2-hydroxy-4,6-dimethylpyrimidine in nicarbazin, Chemom. Intell. Lab. Syst. 150 (2016) 1–8.
[25] J.C. Esteves da Silva, R. Tauler, Multivariate curve resolution of synchronous fluorescence spectra matrices of fulvic acids obtained as a function of pH, Appl. Spectrosc. 60 (2006) 1315–1321.
[26] M.R. Alcaráz, A.V. Schenone, M.J. Culzoni, H.C. Goicoechea, Modeling of second-order spectrophotometric data generated by a pH-gradient flow injection technique for the determination of doxorubicin in human plasma, Microchem. J. 112 (2014) 25–33.
[27] R.I. Shrager, Chemical transitions measured by spectra and resolved using singular value decomposition, Chemom. Intell. Lab. Syst. 1 (1986) 59–70.
[28] W. Windig, J. Guilment, Interactive self-modeling mixture analysis, Anal. Chem. 63 (1991) 1425–1432.
[29] MATLAB 7.6, The MathWorks Inc., Natick,Massachussets, USA, 2008.
[30] J. Reijenga, A. van Hoof, A. van Loon, B. Teunissen, Development of methods for the determination of pKa values, Anal. Chem. Insights 8 (2013) 53–71.
[31] A.D. Kashuba, J.R. Dyer, L.M. Kramer, R.H. Raasch, J.J. Eron, M.S. Cohen, Antiretroviral-drug concentrations in semen: implications for sexual transmission of human immunodeficiency virus type 1, Antimicrob. Agents Chemother. 43 (1999) 1817–1826.
[32] A. Avdeef, Cocrystal solubility product analysis – dual concentration-pH mass action model not dependent on explicit solubility equations, Eur. J. Pharm. Sci. 110 (2017) 2–18.
[33] G. Kuminek, N. Rodriguez-Hornedo, S. Siedler, H.V. Rocha, S.L. Cuffini, S.G. Cardoso, How cocrystals of weakly basic drugs and acidic coformers might modulate solubility and stability, Chem. Commun. (Camb.) 52 (2016) 5832–5835.
[34] L.E.V. Salgado, C. Vargas-Hernandez, Spectrophotometric determination of the pKa, isosbestic point and equation of absorbance vs. pH for a universal pH Indicator, Am. J. Anal. Chem. 5 (2014) 1290–1301.
[35] V. Gómez, M. Miró, M.P. Callao, V. Cerdà, Coupling of sequential injection chromatography with multivariate curve resolution-alternating least-squares for enhancement of peak capacity, Anal. Chem. 79 (2007) 7767–7774.
[36] A.C. Olivieri, Practical guidelines for reporting results in single- and multi-component analytical calibration: a tutorial, Anal. Chim. Acta 868 (2015) 10–22.
[37] M.C. Bauza, G.A. Ibañez, R. Tauler, A.C. Olivieri, Sensitivity equation for quantitative analysis with multivariate curve resolution-alternating least-squares: theoretical and experimental approach, Anal. Chem. 84 (2012) 8697–8706.
[38] K.O. K'Oreje, L. Vergeynst, D. Ombaka, P. De Wispelaere, M. Okoth, H. Van Langenhove, K. Demeestere, Occurrence patterns of pharmaceutical residues in wastewater, surface water and groundwater of Nairobi and Kisumu city, Kenya, Chemosphere 149 (2016) 238–244.
[39] O.A. Abafe, J. Späth, J. Fick, S. Jansson, C. Buckley, A. Stark, B. Pietruschka, B.S. Martincigh, LC-MS/MS Determination of Antiretroviral Drugs in Influents and Effluents from Wastewater Treatment Plants in KwaZulu-Natal, South Africa, Chemosphere, 2018, http://dx.doi.org/10.1016/j.chemosphere.2018.1002.1105 (in press).